International Conference
ENGINEERING MECHANICS 2010
Svratka, Czech Republic, May 10 – 13, 2010

WATER IMPACT MEASUREMENT OF TWO OVERLAPPING HIGH PRESSURE FLAT JET NOZZLES USING TWO DIFFERENT METHODS

J. Kvapil, M. Pohanka

Summary: *Descaling of hot rolled plates is typical application for high pressure flat jet nozzles. Row of nozzles with overlapping area at direction of moving hot plate is usually used. Homogeneity of descaling is very important parameter for final quality of the rolled plate. Paper discusses about measurements of impact footprint for single nozzle as well as for two overlapping nozzles. Two different methods were used in measurements. The first method measures impact forces in the free stream. The second method measures impact forces of water stream penetrating through the forming water layer on a test plate. Size of pressure sensor also influences the measurement data. Different dimensions of sensors were used. Measurement data were recalculated by inverse task to so called zero size sensor. Raw measured data as well as sharpened data are presented. The overlapping area is also discussed in this paper.*

1. Introduction

The steel hot rolling process is inseparably linked to the surface oxidation of rolled material at increased temperatures. Hydraulic descaling of a rolled material is a process of removing the oxide from the hot steel surface. Descaled surface quality is fundamental for the total surface quality of a roll product. More information about descaling is introduced in [1]. In Heat transfer and fluid flow laboratory (Brno UT) we are focused on descaling in relation to the heat transfer and quality of steel surface after descaling process. We can use three different types of measurements. The first one is concentrated on measuring of temperature drop when a product is passing under the nozzle. The second type of measurement consists of surface quality evaluation where a defined layer of oxides is sprayed out and its remaining thickness is analyzed. The third is water pressure distribution measurement which is our subject in this article.

2. Measurement theory of pressure distribution

As we mentioned, the hydraulic descaling is very important tool for removing the oxides from the surface of a plate. For this operation we use high pressure flat jet nozzles. By analyzing water impact we get important parameters such as footprint like pressure and shape. For measurement the pressure distribution a pressure sensor of a finite size is used (see Figure 1).

* Ing. Jiří Kvapil, Ing. Michal Pohanka, Ph.D.: Heat Transfer and Fluid Flow Laboratory, Faculty of Mechanical Engineering, Brno University of Technology; Technická 2896/2; 616 69 Brno; tel.: +420 54114 3236; e-mail: kvapil@lptap.fme.vutbr.cz

To compute a real pressure distribution an inverse algorithm have to be used. The size ratio of a nozzle spray spot and the sensor is responsible for the precision of measured data. As the ratio becomes smaller the precision of the measured data is getting worse because of averaging the impact forces.

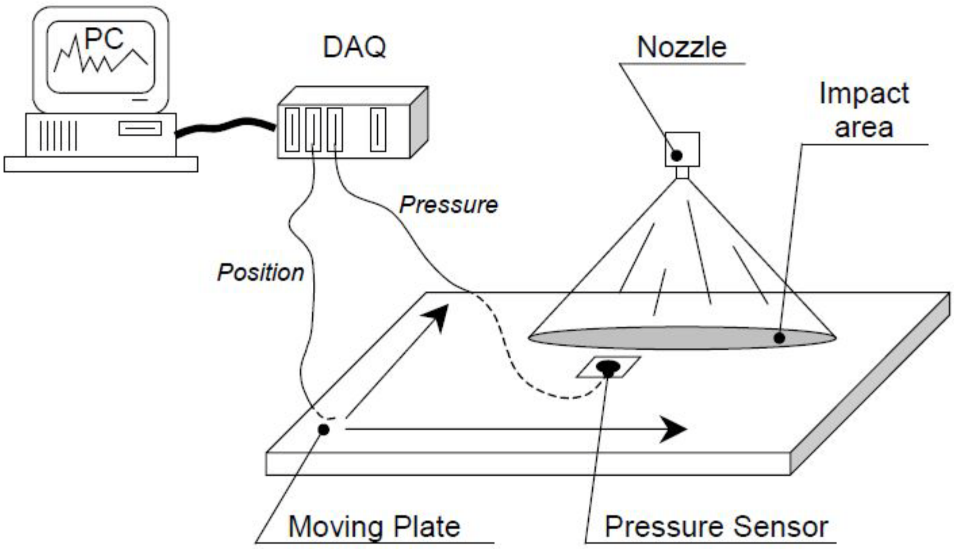

Figure 1 Pressure distribution measurement

This method can creates an inverse pressure sensor after converting data to the frequency domain. We can also multiply the measured data with the inverse pressure sensor and converts the results back to the space domain. Although this method works well also with noisy data, a limit of this method exists.

2.1 Usage of the Fourier transform

For measured data evaluation the Fourier transform (FT) is used. FT is an operation that transforms one complex-valued function of a real variable to another. A physical process can be described either in the space domain, by the values of some quantity h as a function of space x, e.g., $h(x)$, or else in the frequency domain [2], where the process is specified by giving its amplitude H as a function of inverse wavelenght f. We have two functions $h(x)$ and $H(f)$ as two different representations of the same function. One goes back and forth between these two representations by meaning of Fourier transform equations.

$$H(f) = \int_{-\infty}^{\infty} h(x) e^{2\pi i f x} \, dx \quad \textbf{(1)}$$

$$h(x) = \int_{-\infty}^{\infty} H(f) e^{-2\pi i f x} \, df \quad \textbf{(2)}$$

2.2 The Convolution Theorem

The Fourier transform translates between convolution and multiplication of functions. If $h(x)$ and $g(x)$ are integrable functions with Fourier transforms $H(f)$ and $G(f)$, then the Fourier transform of the convolution is given by the product of the Fourier transforms $H(f)$ and $G(f)$. The convolution of the two functions, denoted $g \cdot h$, is defined by

$$y(x) = (g \cdot h)(x) = \int_{-\infty}^{\infty} g(\tau) \cdot h(x - \tau) d\tau \qquad \textbf{(3)}$$

where · denotes convolution operation, then $g \cdot h$ is a function in the time domain and that $g \cdot h = h \cdot g$. It turns out that the function $g \cdot h$ is one member of a simple transform pair

$$g \cdot h \Leftrightarrow G(f) \cdot H(f) \qquad \textbf{(4)}$$

In other words, the Fourier transform of the convolution is just the product of the individual Fourier transforms [2].

2.3 The Discrete Fourier transform (DFT)

It transforms one function into another, which is called the frequency domain representation of the original function. But the DFT requires an input function that is discrete and whose non-zero values have a limited (finite) duration. Such inputs are often created by sampling a continuous function. In the most common situations, function $h(x)$ is sampled (i.e., its value is recorded) at evenly spaced intervals in space. Let Δx denotes the space interval between consecutive samples so that the sequence of sampled values is

$$h_n = h(n\Delta x) \quad n= ..., -3, -2, -1, 0, 1, 2, 3, ...$$

The reciprocal of the space interval Δx is called the sampling rate; if Δx is measured in meters, for example, then the sampling rate is the number of samples recorded per meter.

2.4 The sampling theorem and aliasing

Sampling is the process of converting a signal (for example, function of continuous space) into a numeric sequence (a function of discrete space). For any sampling interval Δx, there is also a special frequency f_c, called the *Nyquist critical frequency* [2], given by

$$f_c \equiv \frac{1}{2\Delta x}$$

The Nyquist critical frequency is important for two distinct reasons. The first one is the remarkable fact known as **the sampling theorem**: If a continuous function $h(x)$, sampled at an interval Δx, happens to be bandwidth limited to frequencies smaller in magnitude than f_c, i.e., if $H(f) = 0$ for all $|f| \geq f_c$, then the function $h(x)$ is completely determined by its samples h_n.

This is a remarkable theorem for many reasons, among them that it shows that the „information content" of a bandwidth limited function is, in some sense, infinitely smaller than that of a general continuous function. The bad news concerns the effect of sampling a continuous function that is not bandwidth limited to less than the Nyquist critical frequency. In that case, it turns out that all of the power spectral density that lies outside of the frequency range $-f_c < f < f_c$ is spuriously moved into that range. This phenomenon is called

aliasing. Any frequency component outside of the frequency range ($-f_c$; f_c) is aliased (falsely translated) into that range by the very act of discrete sampling (see Figure 2).

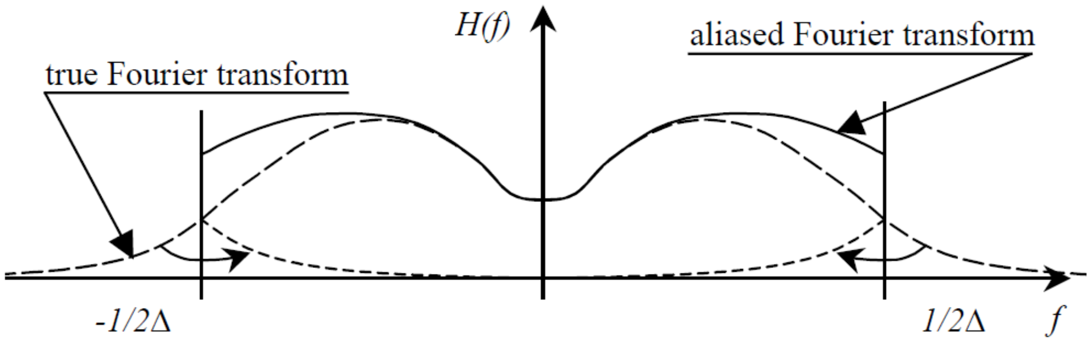

Figure 2 Sampled function translated by the Fourier transform is defined between plus and minus value of the Nyquist critical frequency.

3. Correction of measured data

In fact the measured distribution differs from the real one. Simulated real and measured distribution of pressure is shown in Figure 3. The measured peak is 77.8 MPa, but the real one is 100 MPa. The measured impact shape is wider than the real one. An impact was 20x80 mm and a sensor with circular active surface was assumed [3].

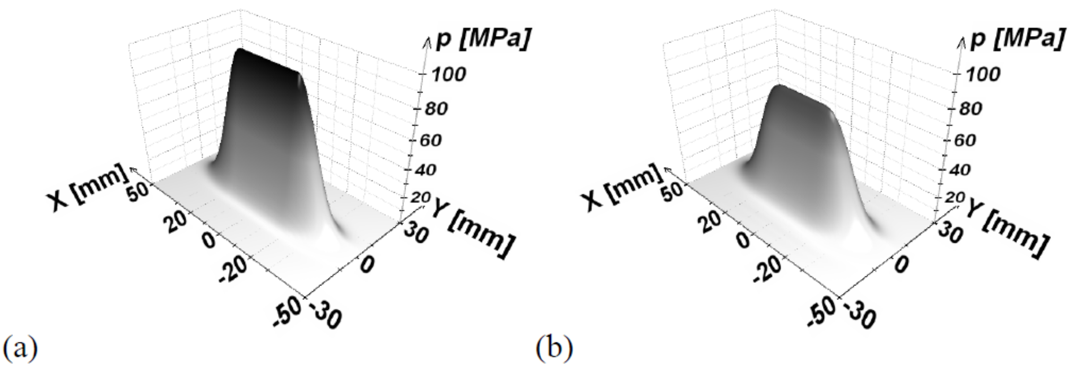

Figure 3 (a) simulated real distribution, (b) simulated measured distribution using a circular sensor of 12 mm in diameter

The diameter active surface was 12 mm. Such a large sensor averages values and one measured value is equal to

$$\bar{p} = \frac{1}{A} \iint_A p(x,y)dxdy \quad \textbf{(5)}$$

where A is the surface of the sensor. The whole measured distribution can be described using the following convolution equation

$$g \cdot h = \iint_A g(x,y) \cdot h(X-x, Y-y)dxdy \quad \textbf{(6)}$$

where *h* is a filter function. This filter function describes how the sensor averages real values. To obtain a real distribution from a measured one, a convolution equation can also be used. In this case, the filter function is an inverse function to the sensor filter function. The convolution, inverse function computation and noise reduction can be done more easily in the frequency domain than in the space domain.

3.1 Conversion to the frequency domain

The data measured using the circular sensor (Ø12 mm) is shown in Figure 3. Measured data and sensor filter function are transformed from the space domain into the frequency domain using FFT (Fast Fourier Transform). A FFT is an efficient algorithm to compute the discrete Fourier transform and its inverse. The transformed values are shown in Figure 4 where the amplitude axes use a logarithmic scale.

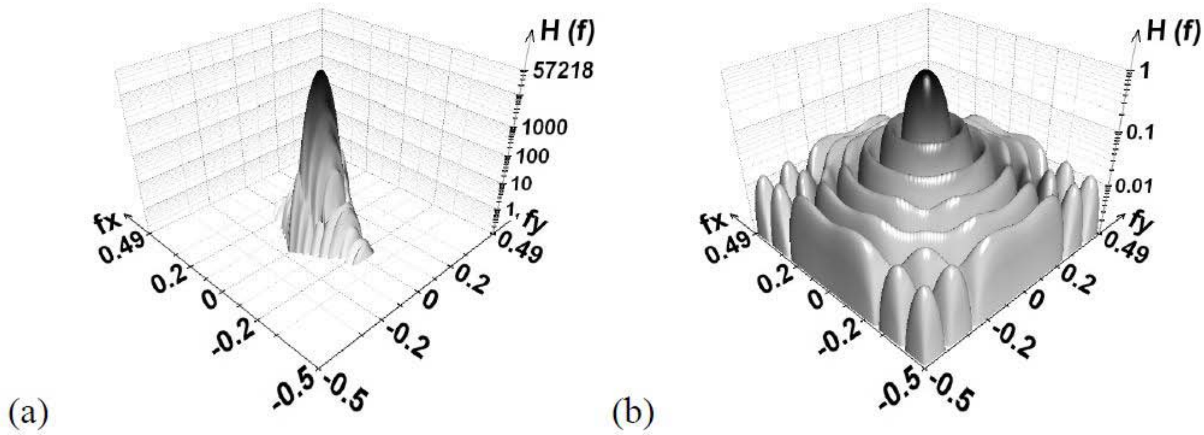

Figure 4 (a) Data in frequency domain, (b) circular sensor in frequency domain.

3.2 Function of Inverse Sensor and Data Sharpening

When the data is transformed into the frequency domain we can compute the inverse sensor filter using

$$h^{-1}(f_x, f_y) = \frac{1}{h(f_x, f_y)} \qquad \textbf{(7)}$$

The inverse sensor filter in the frequency domain is shown in Figure 5a. Having the inverse filter we can do the convolution, eqn (4), in the frequency domain using this inverse filter and measured data to obtain a real pressure distribution (still in the frequency domain), see Figure 5b.

In our case, the convolution is described by

$$S(f_x, f_y) = G(f_x, f_y) \cdot H^{-1}(f_x, f_y) \qquad \textbf{(8)}$$

where G are measured data, H^{-1} is the inverse sensor function and S represents a sharpened data. Transforming sharpened data from the frequency domain into the space domain using inverse FFT we obtain a pressure distribution which should be very close to the real pressure distribution (see Figure 5c). As you can see, some noise is visible in the sharpened data (small waves). Noise can be partially suppressed as described in the following section.

3.3 Noise reduction and aliasing phenomenon

Noise is an unwanted perturbation to a wanted signal. In signal processing or computing it can be considered unwanted data without meaning. Data that is not being used to transmit a signal is simply produced as an unwanted by-product of other activities. In our case noise is the most significant at high frequencies and because we are working in the frequency domain, noise can be suppressed. As you can see in Figure 4b, the sensor function consists of the main frequency spectrum (the highest peak in the middle) and higher harmonic frequencies (the other waves). Cutting off the higher harmonic frequencies and making them equal to zero also in the inverse sensor filter, we get a cut inverse sensor filter. Using this filter for convolution (Eq. 8) instead of the inverse filter and transforming sharpened data using inverse FFT, we get sharpened measured data with suppressed noise. The computed maximum is not 100 MPa but only 96.3 MPa. This is due to the aliasing effect that is described in previous sections. The sampling continuous function that is not bandwidth limited to less than the Nyquist critical frequency results in an incorrect frequency spectrum.

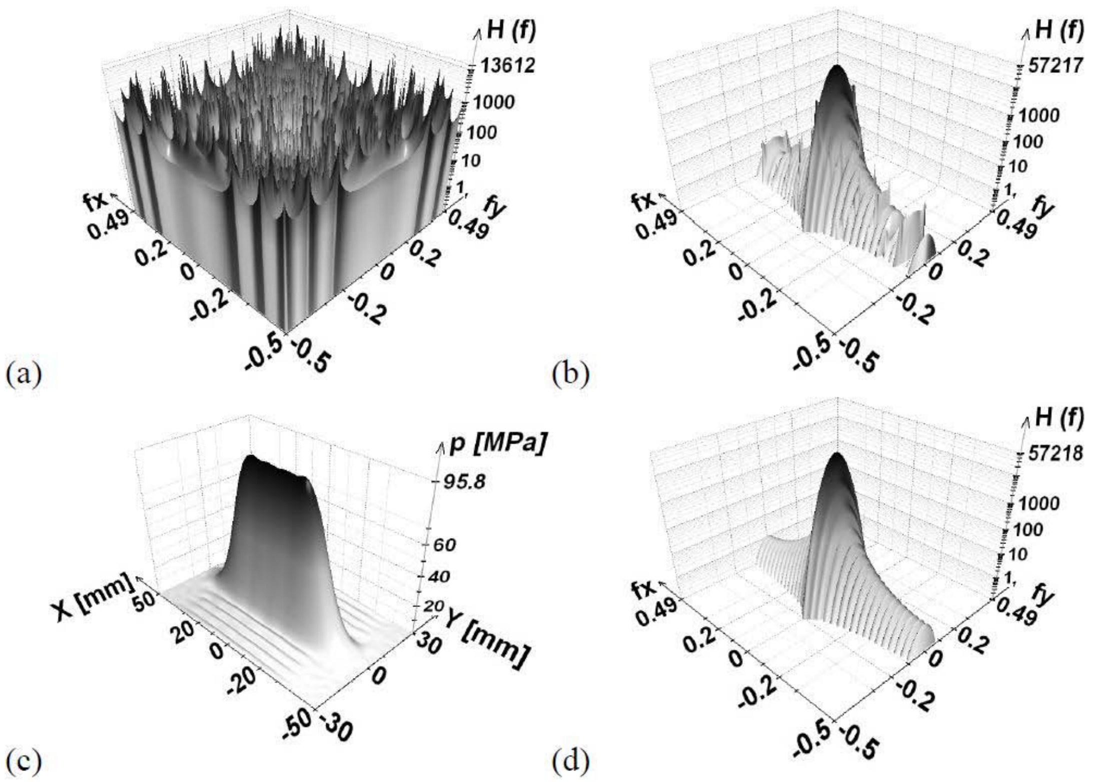

Figure 5 (a) Inverse sensor function in frequency domain; (b) convolution of measured data and inverse sensor function in frequency domain; (c) sharpened measured data – convolution of measured data and inverse sensor function in frequency domain; (d) real pressure distribution in frequency domain.

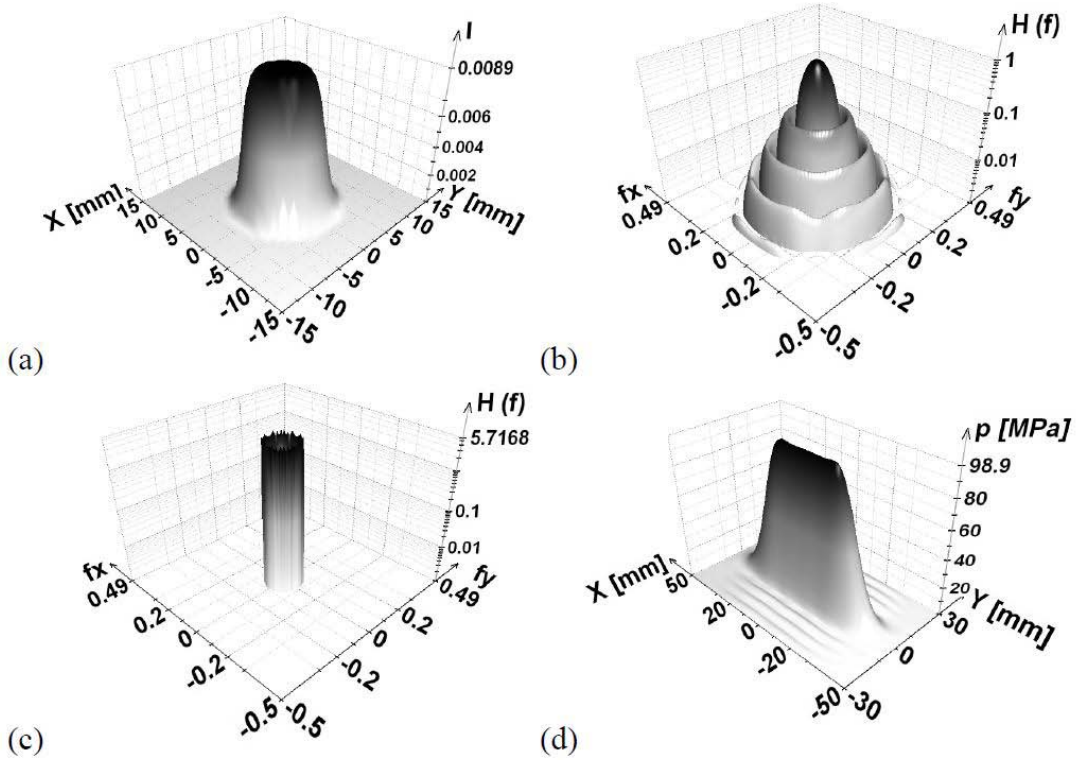

Figure 6 (a) Circular sensor function in space domain filtered using low-pass filter; (b) circular sensor function in frequency domain with removed high frequency; (c) cut inverse sensor function in frequency domain; (d) sharpened measured data.

Any frequency component that lies outside of the range $-f_c < f < f_c$ is spuriously moved into that range (this phenomenon is called **aliasing**). This effect is more significant for the sensor function because of sharp edges of the sensor. All we can do to avoid aliasing is to use a low-pass filter. The sensor function passes through the Gaussian low-pass filter in the space domain. A smoothed sensor function is shown in Figure 6a. Transforming this function into the frequency domain (see Figure 6b), we get high frequencies equal to zero. This means there is no aliasing effect. Using the cut smooth inverse sensor filter for convolution (see Figure 6c) and transforming sharpened data using inverse FFT, we get sharpened measured data (see Figure 6d) with a maximum of 98.9 MPa which is very close to the real maximum 100 MPa. You can also notice that the noise is well suppressed compared with the computed result shown in Figure 5c.

4. Methods of measurement

The measurement was made for high-pressure flat jet nozzle where the distance from the surface was 150 mm and water pressure was 25 MPa. Two different types of measurements are used. The first type measures impact forces in the free stream and the second type measures impact forces under the forming water layer on the sprayed plate.

4.1 Measurement in the free stream

The first type of measurement is based on the pressure sensor that is above the surrounding surface. No water layer is forming during this measurement on the pressure sensor. The main body that holds the pressure sensor has V-shape that allows measurement of flow in the free stream (Figure 7). The sensor has circular shape and 2 mm in diameter. Device contains the dynamometer with max load 5N that measures forces of impinging water from flat jet nozzle. This force is recalculated to impact pressure knowing the dimension of active area of the pressure sensor. Data from the measurement are displayed as 3D chart (See Figure 8). From this chart we can see the specification of the nozzle as footprint, max pressure and detect deficiencies of the nozzle.

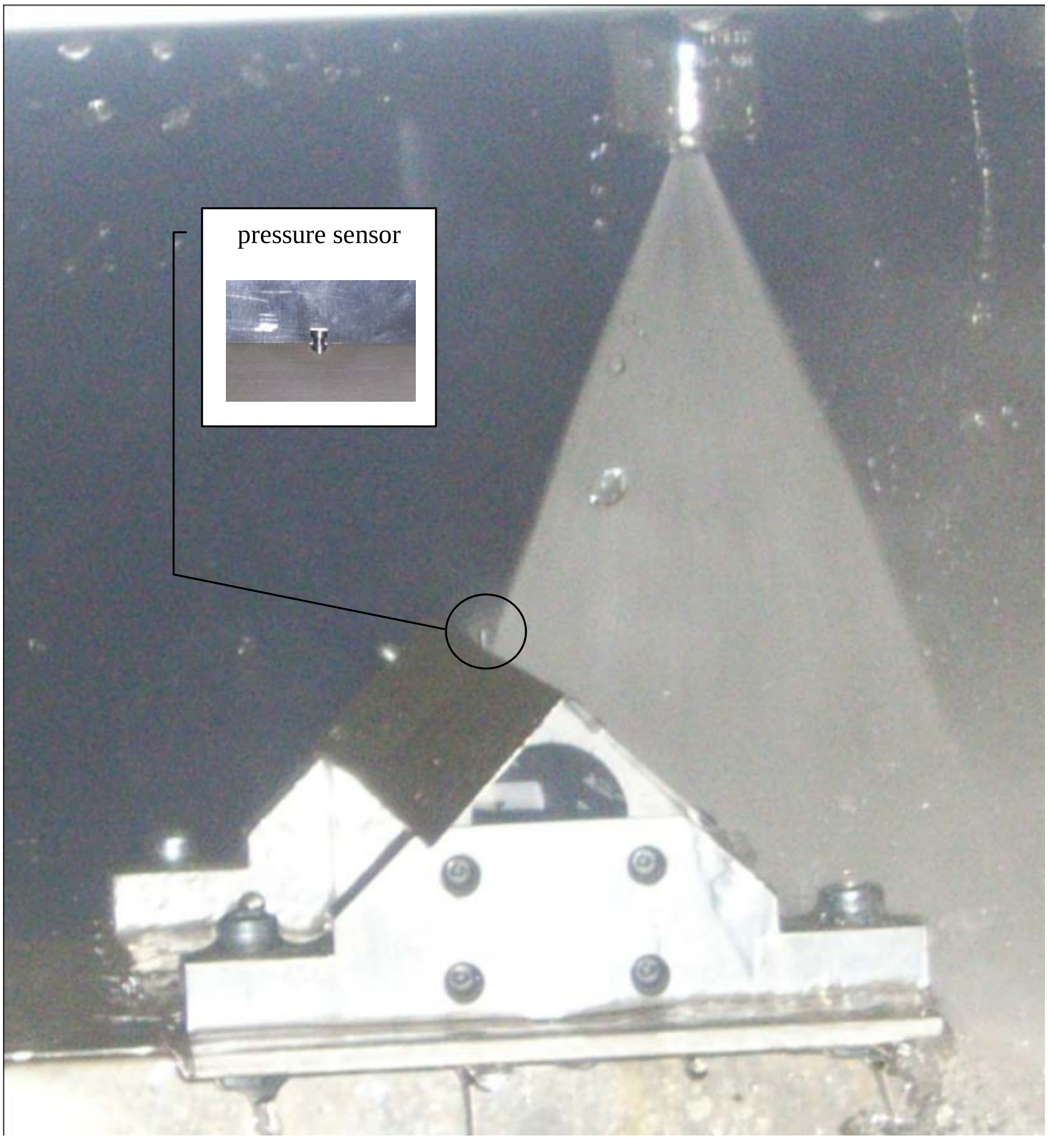

Figure 7 Measuring of water impact in the free stream

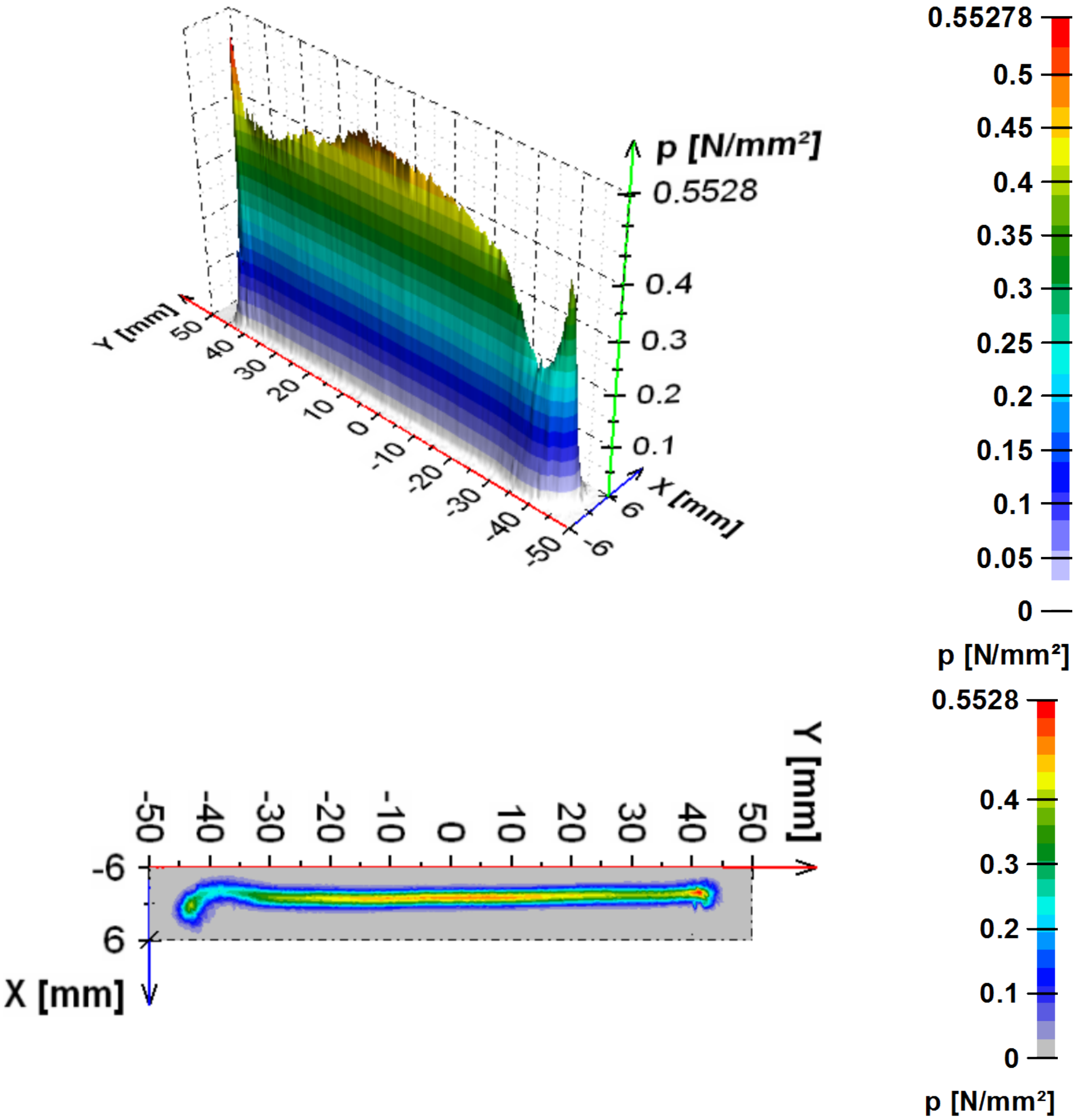

Figure 8 Raw data from measurement in the free stream

4.1.1 Two overlapping nozzles in the free stream

The nozzle in the right position in Figure 9, the fine “teeth” on the record is caused by the scanning step. Scanning step could be reduced but one measurement last over two hours even with this scanning step. Also we can see that the footprint of nozzle in right position is the same as footprint of nozzle in Figure 8. No interactions observed between two overlapping nozzles in the measurement.

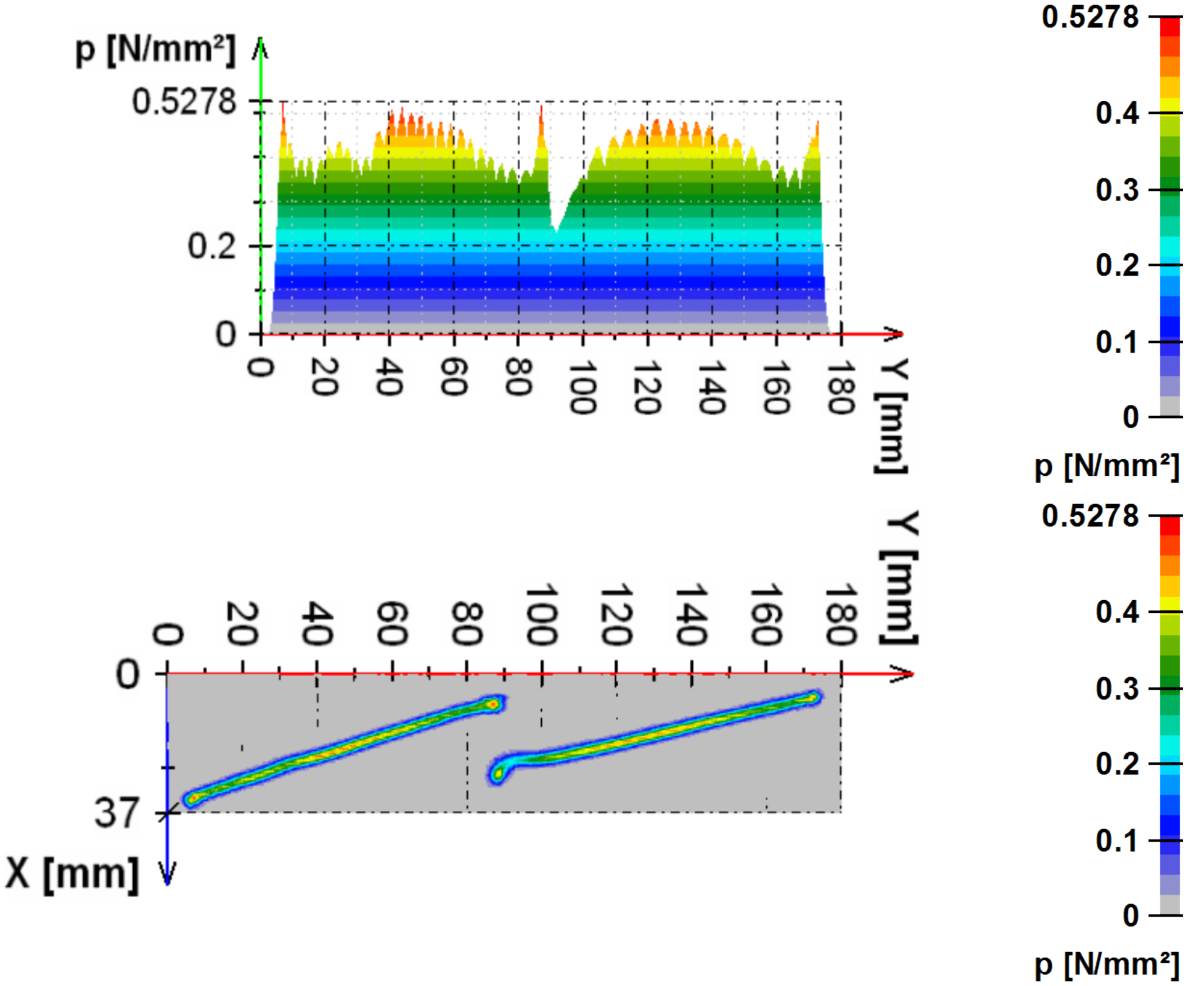

Figure 9 Raw data from measurement of the overlapping nozzles in the free stream

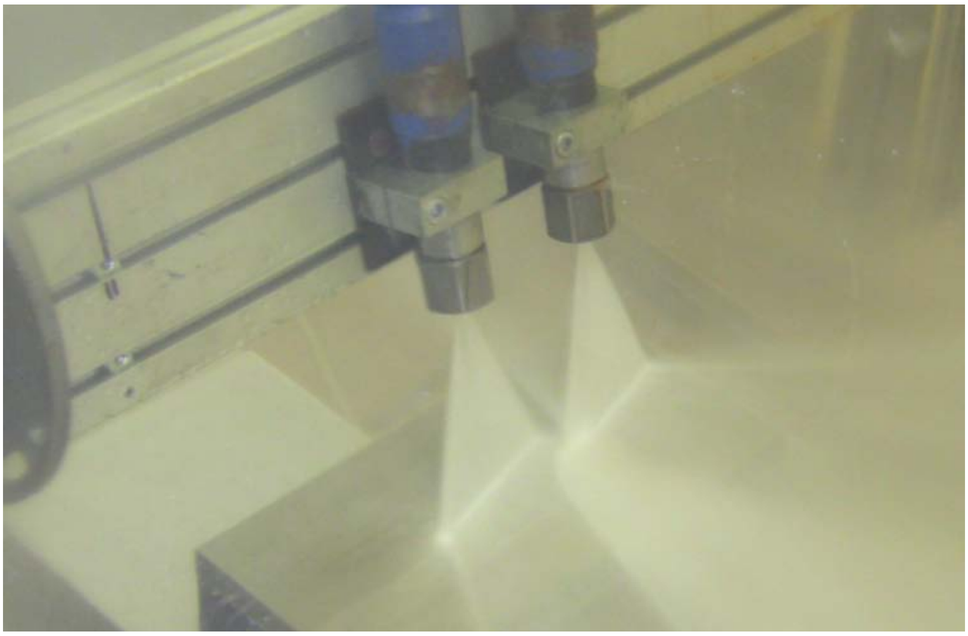

Figure 10 Measurement by the pressure sensor embedded to the test plate

4.2 Measuring with the pressure sensor embedded to the test plate

The second method measures impact forces of water stream penetrating through the forming water layer on the test plate (Figure 10). The pressure sensor is leveled with the plate surface and has 1.5 mm in a diameter. During this measurement the water layer is formed and the pressure sensor in this case measures impact pressure under this water layer. Raw measured data is presented in Figure 11.

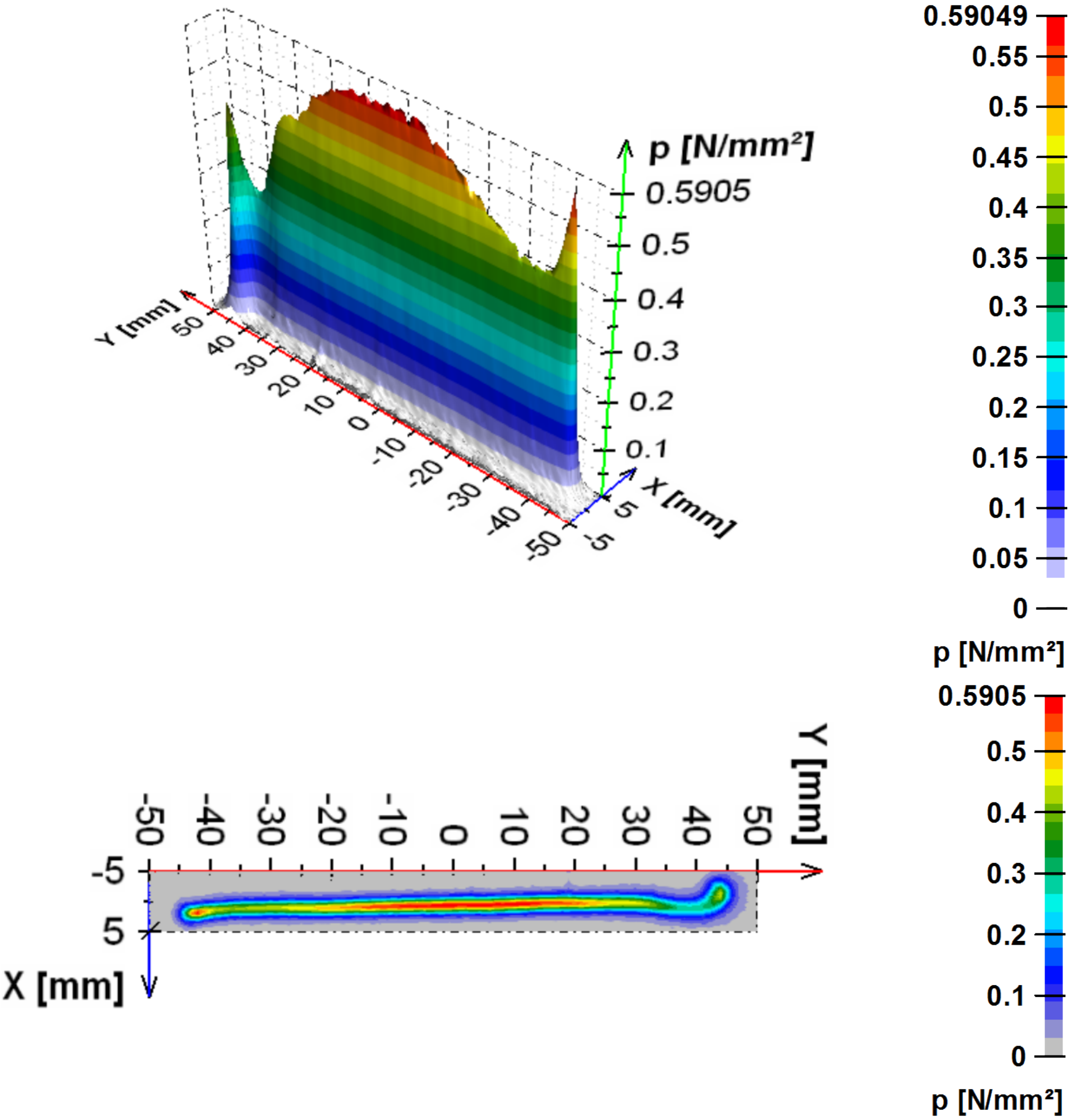

Figure 11 Raw data from measurement by the test plate

4.2.1 Two overlapping nozzles and their interactions under the forming water layer

We concentrate on the two overlapping nozzles. One nozzle does not influence the second nozzle. This is obvious from comparison of measurements shown on Figure 11 and 12. Footprint of the single nozzle in Figure 11 is the same as footprint right nozzle in Figure 12. From this behavior we deduce that the second nozzle does not influence the first nozzle.

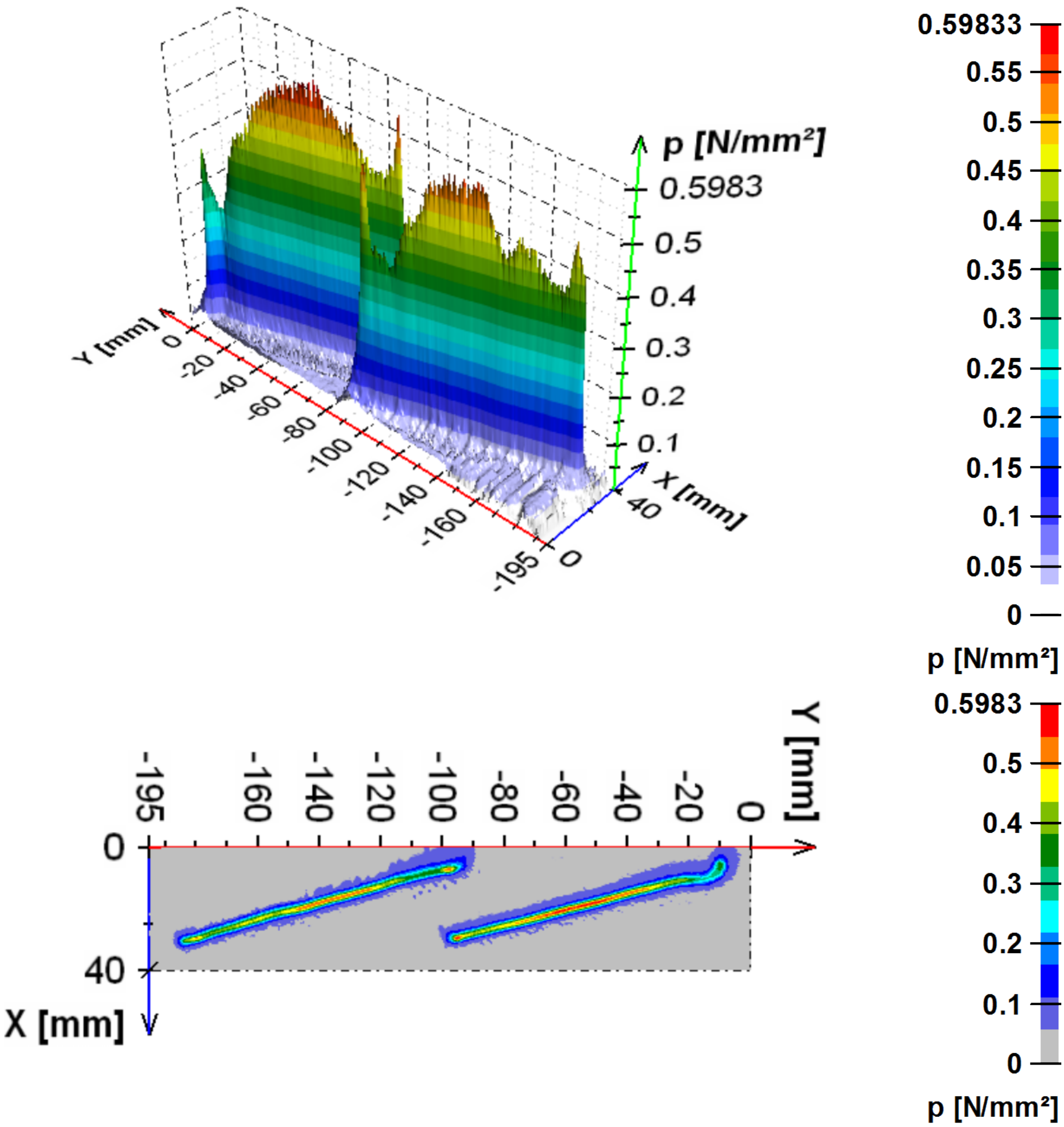

Figure 12 Raw data of two overlapping nozzles from the test plate measurement

5. Filtering and sharpening of the real measured data

Real data from the measurement in the free stream are shown in Figure 8 and from the measurement from the test plate in Figure 11. Some noise in measured data is obvious. Our sharpening algorithm also includes shifting of the pressure distribution to the line that is collinear with axis Y as we look at Figure 13. If we compare Figure 8 and 13 we can see that the pressure maximum is higher in Figure 13. For comparison we attach sharpened data from the measurement on the test plate (Figure 14).

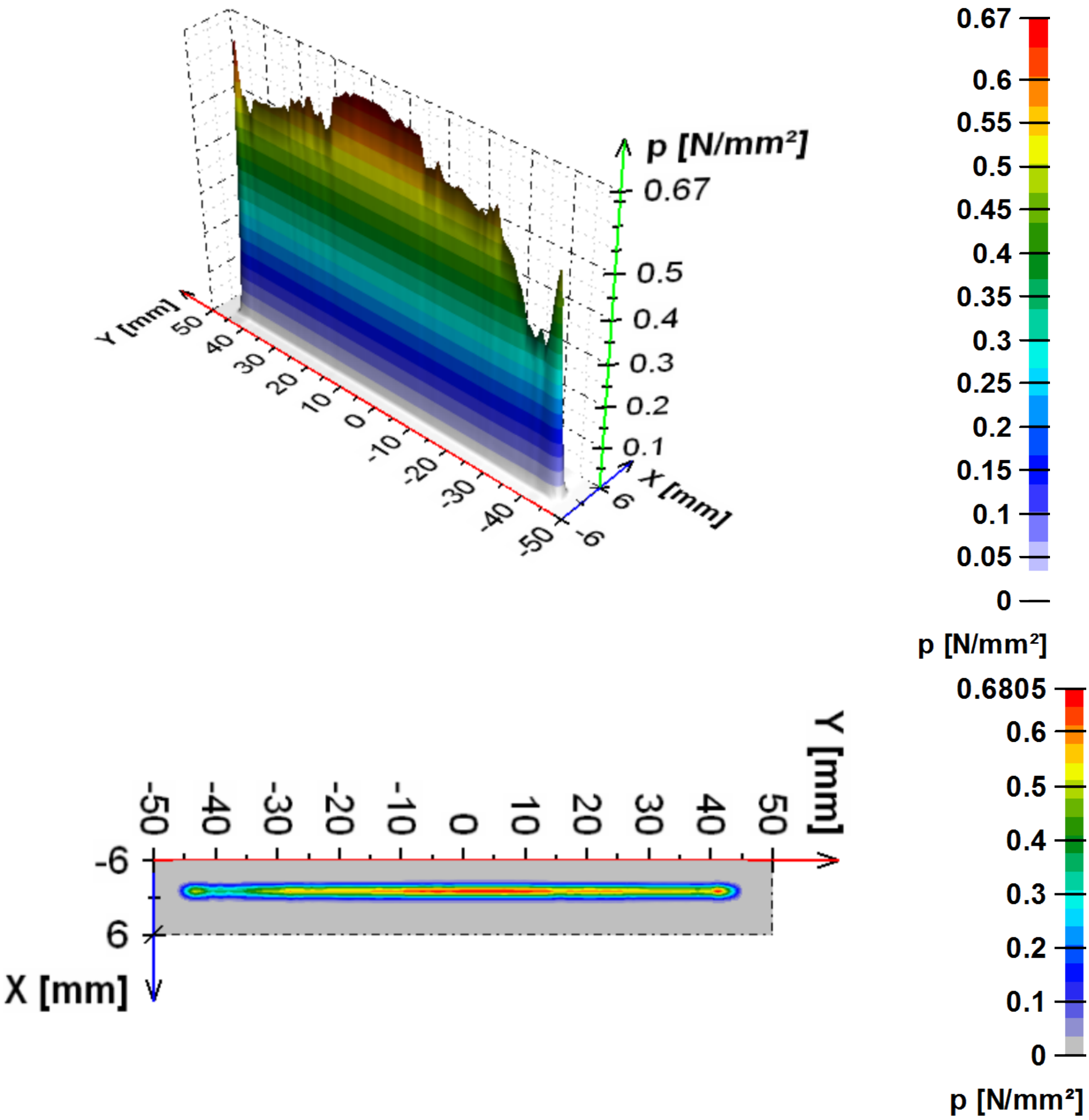

Figure 13 Sharpened data from measurement in the free stream

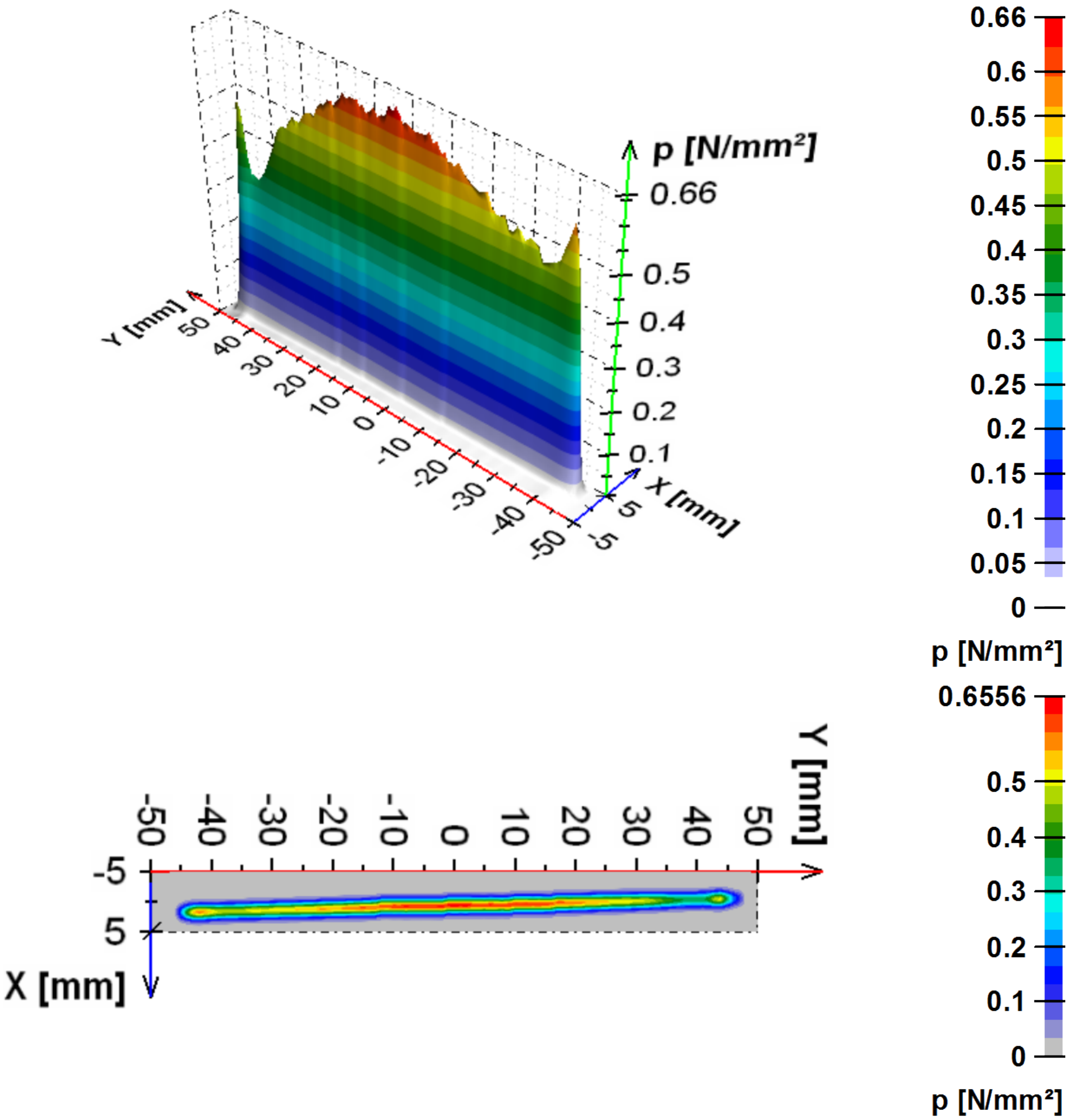

Figure 14: Sharpened data from measurement on the test plate

6. Conclusion

It was shown that any measured data are biased due to the finite size of the measuring sensor. The distortion becomes higher as the size ratio of a nozzle spray spot and the sensor decreases. An inverse method that computes real pressure distribution from measured data has been presented. The presented method works well with any shape of the measuring sensor. During the measurements with sensor embedded in the plate no influence of impact pressure was observed in the overlapping area. Measurements in the free stream and on the test plate were recomputed from sensor size 2.0 mm and 1.5 mm, respectively, to "zero size sensor". The computed maximum values are similar (see Figure 13 and Figure 14). Visual observation of impact on flat surface shows some influence in the overlapping area (see Figure 10) but the measurements did not prove significant effect on the impact water pressure in the interference area.

7. References

[1] Blazevic D., Hot strip mill operation. Vol. VI: Descaling, Sun Lakes, Arizona, U.S.A., 2008.

[2] Press, W. H., Teukolsky, S. A., Vetterling, W. T., Flannery, B. P., *Numerical Recipes in C, The Art of Scientific Computing,* Second Edition, Cambridge University Press, pp. 496-536, 1992.

[3] Pohanka, M. Two-dimensional correction of data measured using a large pressure sensor. *In Computational methods and experimental measurements XI. Halkidiki*: WIT Press, pp. 587–596, 2003.